Fabrication and Characterization of Uranium Oxide Doped Sol−Gel Planar Waveguides for Attenuated Total Reflectance Spectrometry

Paul L. Edmiston and S. Scott Saavedra*

Department of Chemistry, University of Arizona, Tucson, Arizona, 85721

Received June 16, 1997. Revised Manuscript Received September 2, 1997[⊗]

Planar integrated optical waveguides doped with fluorescent hexavalent UO_2^{2+} ions were fabricated by a sol−gel dip-coating process. Excitation of a mode in these waveguides produced fluorescence emission that decayed in a highly uniform manner as a function of propagation distance. A comparison of methods for determining waveguide attenuation coefficients by digital photography of the mode demonstrated that imaging the UO_2^{2+} fluorescence emission is significantly more precise than imaging the Rayleigh and Mie scattered light. The utility of these waveguides for performing attenuated total reflectance measurements on substrate-supported molecular films was also assessed. Both the fluorescence and scattering methods were used to determine the attenuation coefficient of an adsorbed heme protein monolayer. The fluorescence imaging method was clearly superior; its use enables attenuation measurements of very weakly absorbing, waveguide-supported films to be performed with significantly improved precision.

Introduction

A planar integrated optical waveguide (IOW) is a substrate-supported, dielectric film, typically less than 1 μm thick, in which light propagates via total internal reflection in one or a few discrete modes.[1] Relative to a conventional (i.e., much thicker) waveguide, an IOW supports a very high density of reflection sites per unit propagation length (using a ray optics approximation[2a]), which makes these devices particularly useful for evanescent spectral analysis of thin films[2−8] and optically based chemical sensing.[9−12] In many of these applications, measurements are performed by quantitating the attenuation of light propagating in the guided mode due to absorption of the evanescent field by a thin adlayer of chromophores at the IOW−superstrate interface.[2,4,6−8,12]

One method used to measure mode attenuation in an IOW is to outcouple the light using a prism or diffraction grating and measure the intensity using a photodetector.[2] Limitations of this method result from the fact that IOW attenuation measurements are usually conducted in a single-beam geometry. Therefore, a separate, simultaneous measurement must be performed to correct for fluctuations in source power. Furthermore, the efficiency of coupling light into an IOW mode is highly sensitive to variations in the incidence angle of the source beam. When performing attenuation measurements in different modes, which is required in the case of dichroic ratio measurements,[2a,6−8] the incident angle must be varied because the incoupling angle is mode-dependent. Thus waveguide attenuation experiments in which outcoupled mode intensity is measured can be subject to reproducibility problems.

An alternative method to measure attenuation in an IOW is to use a digital camera to photograph the light scattered from the mode as it propagates through the waveguide.[3,13] The instrumental arrangement is depicted in Figure 1. The attenuation coefficient of the mode is proportional to the slope of the curve generated by plotting scatter intensity against propagation distance.[13] Relative to the first method, the imaging method is advantageous because variations in propagating beam intensity due to source intensity fluctuations and incidence angle variations do not affect the measurement since the slope of the curve is independent of scattered light intensity.

However, the imaging method can be problematic when scattered light from the waveguide is spatially nonuniform. The light that is detected results from Rayleigh or Mie scattering by defects within the waveguide volume and surface roughness at the waveguide-cladding interfaces. Variations in scattering efficiency over the propagation length of the IOW are observed as noise spikes, or a nonuniform slope, in the attenuation curve. Particularly problematic is the case

* Corresponding author: Phone (520) 621-9761. FAX (520) 621-8407. sssaaved@ccit.arizona.edu.

[⊗] Abstract published in *Advance ACS Abstracts,* October 15, 1997.

(1) Kogelnik, H. In Topics in Applied Physics 7. *Integrated Optics*; Tamir, T., Ed.; Springer-Verlag: Berlin, 1979; Chapter 2.
(2) (a) Saavedra, S. S.; Reichert W. M. *Anal. Chem*. **1990**, *62*, 2251. (b) Saavedra, S. S.; Reichert, W. M. *Langmuir* **1991**, *7*, 995.
(3) Walker, D. S.; Reichert, W. M.; Berry, C. J. *Appl. Spectrosc.* **1992**, *46*. 1437.
(4) Hughes, K. D.; Bohn P. W. *Appl. Opt.* **1991**, *30*, 4406.
(5) Stayton, P. S.; Ollinger, J. M.; Jiang, M.; Bohn, P. W.; Sliger, S. G. *J. Am. Chem. Soc.* **1992**, *114*, 9298.
(6) Lee, J. E.; Saavedra, S. S. In *Proteins at Interfaces II*; Horbett, T. A., Brash, J. L., Eds.; ACS Symposium Series 602; American Chemical Society: Washington, DC, 1995; p 269.
(7) Lee, J. E.; Saavedra, S. S. *Langmuir* **1996**, *12*, 4025.
(8) Edmiston, P. L.; Lee, J. E.; Wood, L. L.; Saavedra, S. S. *J. Phys. Chem*. **1996**, *100*, 775.
(9) Giuliani, J. F.; Wohltjen, H.; Jarvis, N. L. *Opt. Lett.* **1983**, *8*, 54.
(10) Carlyon, E. E.; Lowe, C. R.; Reid, D.; Bennion, I. *Biosens. Bioelectron*. **1992**, *7*, 141.
(11) Stewart, G.; Culshaw, B. *J. Quantum Electron*. **1994**, *26*, S249.
(12) (a) Yang, L.; Saavedra, S. S. *Anal. Chem*. **1995**, *67*, 1307. (b) Yang, L.; Saavedra, S. S.; Armstrong, N. R. *Anal. Chem*. **1996**, *68*, 1834.
(13) Yang, L.; Saavedra, S. S.; Armstrong, N. R.; Hayes, J. *Anal. Chem*. **1994**, *66*, 1254.

S0897-4756(97)00429-8 CCC: $14.00

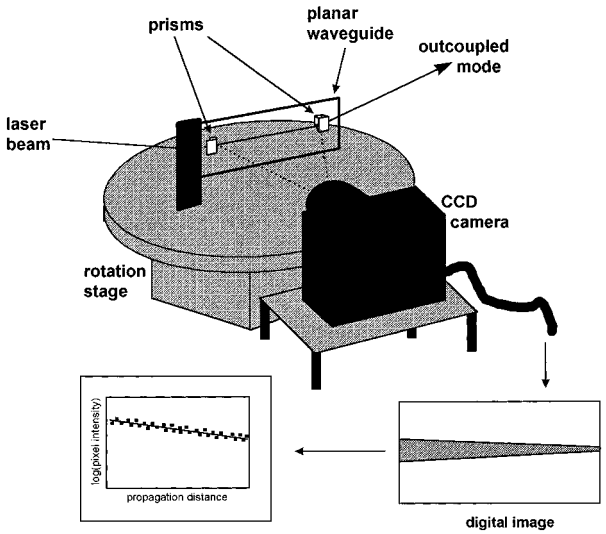

Figure 1. Schematic of the instrumental arrangement for measuring the attenuation curve of a planar waveguide using digital photography. Prisms are used to couple light in to and out of the waveguide mode. The scattered light or fluorescence generated from the propagating mode between the prisms is imaged using a CCD camera oriented normal to the waveguide plane. The digital image is vertically averaged and the data are plotted as the log of the intensity vs propagation distance.

when several relatively large defects (>1 μm), each of which generates a high-intensity scattering spike, are present within a 2−3 cm propagation length of a waveguide mode. In such a case, the precision in determining the slope of the attenuation curve can be significantly compromised.

One strategy to overcome this problem is to image a secondary emission process excited by the waveguide mode, such as fluorescence. In the absence of significant self-quenching, emission intensity is directly proportional to excitation intensity and thus also to mode attenuation as a function of propagation distance.[14]

In previous papers, we described the fabrication and characterization of low-loss, sol−gel derived IOWs[13] and the use of IOWs to quantitate evanescent absorption, via scattering measurements, by an organic adlayer at the IOW−superstrate interface.[6−8,15−16] In principle, the sol−gel method provides a facile route for introducing dopants into the IOW if the dopant can be dissolved in the sol from which the waveguide coating is applied and is stable under the conditions required for thermal densification of the gel. Described here is fabrication and characterization of sol−gel derived, fluorescent IOWs which we have developed to improve the precision of IOW attenuation measurements. Hexavalent UO_2^{2+} ions are used as the fluorescent dopant. The physical and spectral characteristics of UO_2^{2+}-doped waveguides are reported, and their use for IOW-based linear dichroism experiments is evaluated. Imaging fluorescence emission as a function of guided mode propagation distance is shown to be an improved method, relative to imaging scattered light, for determining absorption by IOW-supported films.

(14) Okamura, Y.; Sato, S.; Yamamoto, S. *Appl. Opt.* **1985**, *24*, 57.
(15) (a) Edmiston, P. L.; Lee, J. E.; Cheng S. S.; Saavedra, S. S. *J. Am. Chem. Soc.* **1997**, *119*, 560. (b) Wood, L. L.; Cheng, S.-S.; Edmiston, P. L.; Saavedra, S. S. *J. Am. Chem. Soc.* **1997**, *119*, 571.
(16) Edmiston, P. L.; Saavedra, S. S., manuscript in review.

Experimental Section

Waveguide Fabrication. Soda-lime glass slides (Gold Seal; Becton, Dickenson, and Co.) used as substrates for the sol−gel waveguides were cleaned by light mechanical scrubbing with a cotton pad in a 1% (v/v) aqueous solution of PCC-54 detergent (Pierce). The slides were then rinsed, sonicated for 15 min, and rinsed again in deionized water (type I reagent grade). Prior to dip-coating, the slides were allowed to air-dry overnight uncovered in a class 1000 laminar flow hood.

Sol−gel solutions were prepared in 1000 mL glass jars that were first cleaned with 1% PCC-54 solution and dried at 200 °C for 30 min. The following reagents were added sequentially: 200 mL of ethanol (100%, Quantum Chemical), 150 mL of methyltriethoxysilane (Aldrich), 75 mL of titanium tetrabutoxide (Aldrich), and 20 mL of silicon chloride (Aldrich). The silicon chloride was added using a syringe to inject the reagent under the surface of the solution. The resulting transparent, light yellow solution was mixed for 10 min before 100 mg of uranyl(VI) acetate dihydrate (Baker Analytical) was added. (**Caution**: Appropriate handling and disposal procedures for radioactive reagents should be followed.) The jar was sealed, and the solution was mixed for 15 min and then allowed to cool to room temperature before being used for IOW fabrication.

Sol−gel waveguides were fabricated using a procedure similar to that described by Yang et al.[13] The slide was mounted on a dipping apparatus, lowered into the sol−gel solution at a rate of 25 cm/min, withdrawn at the same rate, and immediately annealed in a tube furnace at 500 °C in air for 18−25 min. The waveguide was then removed slowly from the furnace to prevent cracking (which occurred if cooling was too rapid). All manipulations were carried out in a class 1000 laminar flow hood at an ambient temperatures and relative humidity levels between 21 and 27 °C and 45 and 60%, respectively. (Note that relative humidity < 45% is also satisfactory for waveguide fabrication.)

Waveguide Characterization. Waveguide modes were excited via prism coupling using the 514.5 nm beam from an Ar^+ laser (Coherent Innova 70). The thickness and refractive index of waveguides were determined by measuring the TE_0 and TM_0 incoupling angles, assuming a step profile for the IOW index and an index of $n = 1.51$ for the glass substrates.[13] Waveguide propagation loss was analyzed by imaging either the scattered light or the uranyl ion fluorescence of guided modes using a thermoelectrically cooled, charge-coupled device (CCD, Princeton Instruments) oriented normal to the waveguide plane (Figure 1). Scattered light was imaged through a 1 nm band-pass filter centered at 514.5 nm (514DF1, CVI Laser Corp.); fluorescence emission was imaged through a 25 nm band-pass filter centered at 568 nm (568DF25, Omega Optical). For each loss measurement, three photographs were recorded for subsequent averaging. Attenuation curves were generated by plotting the logarithm of the vertically averaged pixel intensity against propagation distance. The slope of each curve was determined by least-squares regression by fitting the data to $I(x) = -(\alpha/10)x + C$, where $I(x)$ is log(average pixel intensity), x is the propagation distance in centimeters, α is the loss coefficient in decibels per centimeter, and C is a constant.

IOW−ATR Absorbance Measurements. Integrated optical waveguide−attenuated total reflectance (IOW−ATR) measurements of horse heart cytochrome *c* adsorbed to dichlorodimethylsilane (DDS, Aldrich) modified, UO_2^{2+}-doped waveguides were performed as described in refs 6, 7, and 15a. Waveguides were first cleaned in an 80 °C Chromerge bath for 30 min, placed in a 1 M nitric acid bath for 1 h, rinsed with deionized water, dried at 200 °C for 30 min, and finally soaked in a 2% (v/v) DDS solution in dry toluene (distilled over sodium) for 2 h. The silanized waveguides were sequentially rinsed with toluene, ethanol, and water and sealed in a container at room temperature until use.

The procedures, instrumental arrangement, and theory for IOW-based measurements have been described in detail in previously[6−8] and are only briefly outlined here. Prior to use, DDS-coated waveguides were mounted in a liquid flow cell,

which was in turn mounted on a high-resolution rotary stage (New England Affiliated Technologies). Phosphate buffer (50 mM, pH 7.2) was injected into the flow cell and incubated for 15 min. The 514.5 nm beam was prism coupled into the TE_0 waveguide mode, which produced a "streak" of fluorescent or scattered light visible in the waveguide. This streak was imaged using the CCD through the 514DF1 band-pass filter to detect the scattered light or the 568DF25 band-pass filter to detect the uranyl ion fluorescence. Three photographs were acquired for subsequent averaging. A 35 μM solution of horse heart cytochrome *c* (Sigma) in phosphate buffer was then injected into the flow cell and allowed to equilibrate with the waveguide surface for 30 min before being flushed with phosphate buffer. Images of the TE_0 polarized mode were again recorded through each band-pass filter. The loss due to absorbance by the adsorbed protein film was calculated from the slopes of the attenuation curves using the theory and procedure described previously.[6−8,15a]

Results and Discussion

To produce a sol−gel derived, fluorescently doped IOW useful for absorption measurements of planar supported organic films, the dopant must (i) be soluble in the sol−gel precursor solution, (ii) be stable at annealing temperatures exceeding 500 °C, (iii) fluoresce with at least moderate quantum yield and be relatively insensitive to photobleaching, and (iv) be capable of being excited at a laser wavelength where the organic adlayer also absorbs light. The high temperatures at which sol−gel films are annealed and the necessary resistance to photobleaching essentially preclude the use of organic fluorophores. On the basis of these criteria, an inorganic ion or complex appears best suited as a fluorescent dopant in sol−gel waveguides. The hexavalent uranyl ion (UO_2^{2+}) has previously been used as an optical probe in sol−gel derived glasses.[17−19] Absorbance of blue light by UO_2^{2+} is due to a charge-transfer transition where an oxygen 2p electron is excited to the empty uranium 5f level. The fluorescence emission spectrum contains several bands that result from radiative decay to several ground-state vibrational levels and have been assigned to symmetric and antisymmetric vibrations of the U−O bond.[20] The relative band intensities are sensitive to the chemical environment of the ion.[21,22]

Waveguide Characterization: The physical properties of the uranium doped sol−gel waveguides are nearly identical with undoped sol−gel waveguides prepared previously in this laboratory.[13] All waveguides allowed propagation of only a single mode. The mean thickness and refractive index of seven representative fluorescent waveguides were 0.561 ± 0.049 μm and 1.585 ± 0.012, respectively. The sol−gel was mechanically hard and resistant to acid and organic solvents and could be surface modified using silane chemistry after a 30 min soak in 80 °C Chromerge. Nearly all of the waveguides fabricated on two separate occasions exhibited modes that traversed the length of the waveguide (>5 cm) using 514.5 nm light. Out of this group, roughly half were considered to be high quality and low loss (≤2 dB/cm), making them useful for IOW−ATR experiments.[23] Particulate contamination of the sol−gel solution was the most typical cause of defects in the remainder of each batch of waveguides. Optical microscopy was used to confirm the absence of cracks in the waveguide structure (on the size scale of several microns or greater).

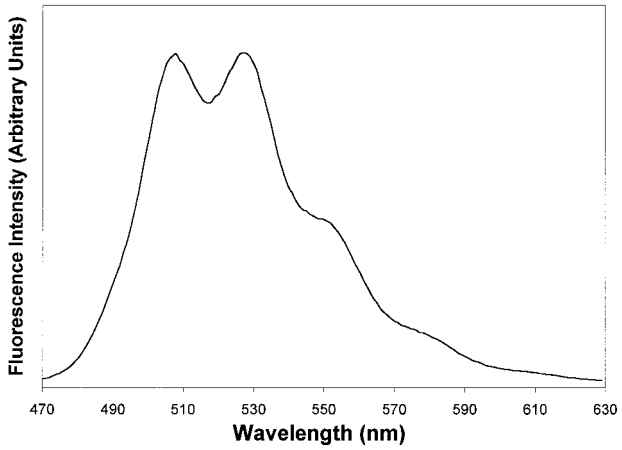

Figure 2. Fluorescence emission spectrum of a UO_2^{2+}-doped, sol−gel derived, planar waveguide excited using the 457.9 nm line of an argon ion laser.

Fluorescence from the UO_2^{2+} waveguides appeared spatially uniform as observed by epifluorescence microscopy. The emission spectrum, acquired on a total internal reflection fluorescence microscope[24] using 457.9 nm laser excitation, is shown in Figure 2. The spectrum consists of broad overlapping bands characteristic of UO_2^{2+} ions doped in sol−gel silica;[17,18] thus during annealing to densify the waveguide, the dopant remains as UO_2^{2+}. Although the excitation maximum was determined to be 430 nm, fluorescence emission could be excited at longer wavelengths. Relative fluorescent intensity versus wavelength of Ar^+ laser line coupled into the TE_0 waveguide mode followed the order: 457.9 > 476 > 488 > 501 > 514.5 nm when normalized to incident laser power. At 457.9 nm noticeable attenuation of the propagating mode was observed due to the absorbance of light by UO_2^{2+} ions, a problem which could be rectified by lowering the doping density.

Waveguide attenuation curves were generated by plotting the logarithm of the vertically averaged pixel intensity in each digital image as a function of propagation distance.[13] Attenuation curves for one waveguide measured by sequentially imaging the scattered laser light and the uranyl fluorescence are shown in Figure 3. The optical quality of this waveguide, with respect to uniformity of propagation loss, is excellent due to the lack of large scattering centers. However, even for this waveguide there is considerable noise in the scattered light curve (Figure 3A), which is likely due to variations in size and shape of microscopic scattering centers in the sol−gel layer. The noise is greatly reduced by

(17) Brandel, V.; Iroulart, G.; Simoni, E.; Genet, M.; Audière, J. P. *New J. Chem.* **1990**, *14*, 133.
(18) McDonagh, C.; Marron, P.; Kiernan, P.; McGlip, J. F. *SPIE Vol. 1758: Sol−Gel Optics II* **1992**, 48.
(19) Pope, E. J. *SPIE Vol. 1758: Sol−Gel Optics II* **1992**, 360.
(20) Leung, A. F.; Lai, T. W. *J. Chem. Phys.* **1982**, *76*, 3913.
(21) Lieblich-Sofer, N.; Reisfeld R. *Inorg. Chim. Acta* **1978**, *30*, 259.
(22) Azenha, M. E. D. G.; Burrows, H. D.; Formosinho, S. J.; Miguel, M. G. M.; Daramanyan, A. P.; Khudyakov, I. V. *J. Lumin.* **1991**, *48−49*, 522.
(23) The sol−gel derived planar waveguides currently being fabricated in our laboratory exhibit higher attenuation coefficients (typically 1 dB/cm) than the attenuation coefficients of ca. 0.1 dB/cm reported in ref 13. However, despite higher overall loss, the uniformity of the loss over the waveguide length is typically better than that achieved using our initial fabrication procedure.
(24) Phimphivong, S.; Kölchens, S.; Edmiston, P. L.; Saavedra, S. S. *Anal. Chim. Acta* **1995**, *307*, 403.

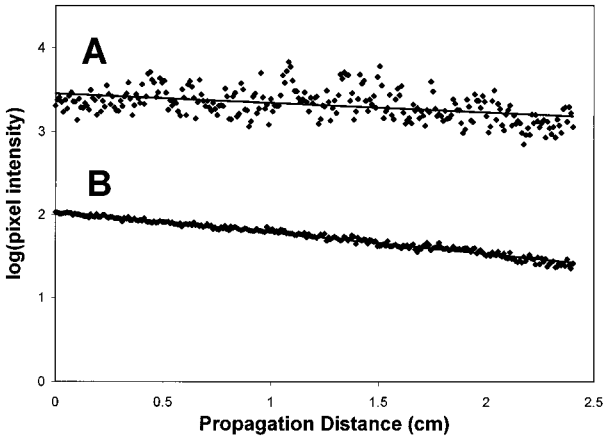

Figure 3. Attenuation curves for a UO_2^{2+}-doped sol−gel waveguide of relatively high optical quality. Solid lines represent the best linear fit using least squares regression. (A) Attenuation data measured by imaging the scattered light from the waveguide mode. The slope of the curve is 1.31 ± 0.10 dB/cm. (B) Attenuation data measured for the same mode by imaging the UO_2^{2+} fluorescence. The slope of the curve is 2.45 ± 0.018 dB/cm.

imaging the uranyl fluorescence, as the curve plotted in Figure 3B illustrates. Using least-squares regression analysis, attenuation coefficients and associated standard errors were calculated. The scattered light curve had a calculated attenuation coefficient of 1.31 ± 0.10 dB/cm, while α for the fluorescence image was 2.45 ± 0.018 dB/cm. Two points are apparent from these data. First, there is a ca. 5-fold reduction in standard error when the attenuation coefficient is determined from the fluorescent image. This is important because absorbance of an adlayer coated on the waveguide surface is measured as increase in α relative to α for the bare waveguide (see below). Second, there is a relatively large difference in the calculated α values, which suggests that measurement of scattered light from a waveguide may lead to an inaccurate determination of the attenuation coefficient.

Attenuation curves measured by sequentially imaging scattered light and uranyl ion fluorescence for a second waveguide are shown in Figure 4. This waveguide is of lower optical quality than the first example. The scattered light attenuation curve (Figure 4A) shows the presence of several bright scattering centers between 0 and 2.5 cm of propagation distance, plus a relatively large scattering structure near 3.5 cm. These scattering centers substantially increase the noise in the curve. Regression analysis from 0 to 3 cm (neglecting the large scattering structure near 3.5 cm) yielded α = 3.38 ± 0.17 dB/cm. The noise in the data is substantially reduced by imaging the uranyl ion fluorescence; α = 1.67 ± 0.025 dB/cm for the curve plotted in Figure 4B. The difference in α values determined from the scattered light and fluorescence attenuation curves again suggests that scattered light imaging may yield inaccurate results. However, this error does not appear to be systematic since for this waveguide, the α value determined by scattered light imaging is greater than that determined by fluorescence imaging, whereas the opposite is true for the first waveguide.

Applicability to Thin-Film Absorbance Measurements. The utility of UO_2^{2+}-doped fluorescent waveguides for IOW−ATR measurements of surface

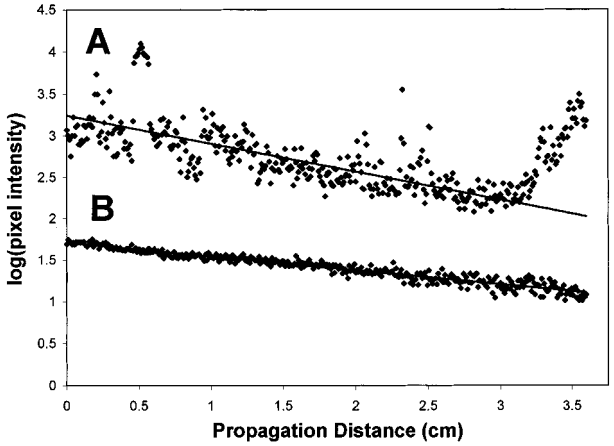

Figure 4. Attenuation curves for a UO_2^{2+} doped sol−gel waveguide of relatively low optical quality which contained several bright scattering centers. Solid lines represent the best linear fit using least squares regression. (A) Attenuation data measured by imaging the scattered light from the waveguide mode. The slope of the curve is 3.38 ± 0.17 dB/cm; the last 0.5 cm was omitted from regression analysis. (B) Attenuation data measured for the same mode by imaging the UO_2^{2+} fluorescence. The slope of the curve is 1.67 ± 0.025 dB/cm.

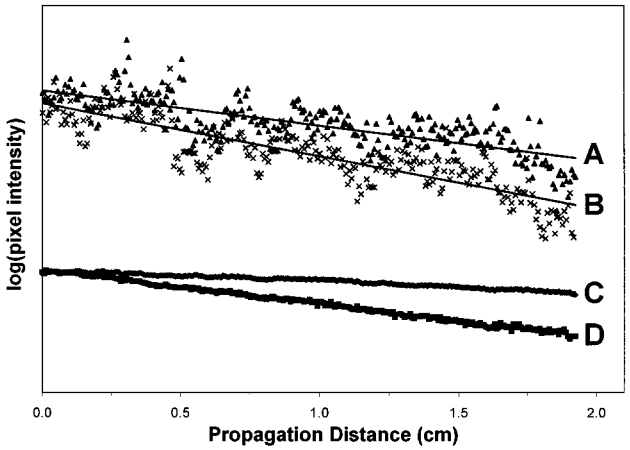

Figure 5. (A and B) Attenuation data for a UO_2^{2+} doped sol−gel waveguide measured by imaging the scattered light from the waveguide mode before and after adsorption of a monolayer of cyt *c*, respectively. (C and D) Attenuation data measured for the same mode by imaging the UO_2^{2+} fluorescence before and after cyt *c* adsorption, respectively. Solid lines represent the best linear fit using least squares regression. Slopes are (A) 3.64 ± 0.19 dB/cm; (B) 5.49 ± 0.20 dB/cm; (C) 1.18 ± 0.012 dB/cm, and (D), 3.51 ± 0.016 dB/cm.

adlayers was assessed by measuring attenuation coefficients for a test sample using both the scattered light and fluorescence imaging methods**.** The test sample was horse heart cytochrome *c* (cyt *c*) adsorbed to a waveguide silanized with DDS. Previous work[7,15a] has shown that under the incubation conditions described above, approximately one monolayer of protein is adsorbed and that the resulting protein film is relatively ordered on a macroscopic scale. In Figure 5 are plotted waveguide attenuation curves measured by imaging the scattered light and uranyl ion fluorescence both before and after adsorption of cyt *c* to the silanized waveguide surface. The attenuation coefficients calculated from the scattered light measurements before and after protein adsorption (curves A and B) were 3.64 ± 0.19 and 5.49 ± 0.20 dB/cm, respectively. The difference, 1.85 ± 0.27 dB/cm, represents attenuation of the mode

due to absorbance by the protein film. As illustrated above, substantially less scatter is observed in the data obtained by fluorescence imaging (curves C and D). The attenuation coefficients before and after protein adsorption were 1.18 ± 0.012 and 3.51 ± 0.016 dB/cm, respectively. The difference between the two values, 2.33 ± 0.02 dB/cm, again is the attenuation coefficient of the protein film.

Thus regardless of the method employed, a similar value is obtained for the attenuation coefficient of the adsorbed protein film (1.85 vs 2.33 dB/cm for scattered light vs fluorescence imaging, respectively). However, this comparison demonstrates that fluorescence imaging is a more precise method than scattered light imaging for determining the absorbance of a waveguide-supported film of chromophores. Curves C and D in Figure 5 are substantially less noisy than curves A and B, which is reflected in a significantly smaller standard error in the protein film attenuation coefficient (0.27 vs 0.02 dB/cm for scattered light vs fluorescence imaging, respectively). Fluorescence imaging has consequently become the preferred method in our laboratory for determining attenuation coefficients of heme protein films deposited on sol−gel derived IOWs. However, since the measurement is performed at a single wavelength, this method cannot be used to resolve competitive adsorption of multiple proteins. The use of a multiwavelength version of IOW−ATR, as reported by Mendes et al.,[25] is a potential solution to this limitation.

Photobleaching. A key aspect in choosing a dopant as a spectroscopic probe to spatially quantitate the amount of light propagating in a waveguide mode is its susceptibility to photobleaching. In the application described in this paper, a dopant that is readily photobleached would be unacceptable. Since the rate of photobleaching of a fluor is proportional to the intensity of light, fluors immobilized in the waveguiding layer near the incoupling prism, where the light intensity is greater, would photobleach faster than those located several centimeters of propagation distance "down" the waveguide. The result would be a systematic reduction in the slope of the attenuation curve over the time course of an experiment. Since inorganic ions and complexes are inherently much more photostable than organic molecules, UO_2^{2+} appeared to be a good choice for preparing fluorescent, sol−gel derived planar IOWs.

To assess the susceptibility of UO_2^{2+} immobilized in a sol−gel layer to photobleaching, the 514.5 nm line of the Ar^+ laser with an incident power of 30 mW was prism coupled into a UO_2^{2+}-doped waveguide. The attenuation coefficient was measured as a function of time during 40 min of continuous illumination and exhibited a nearly linear decline of 17% during this period. The nature of the decline was addressed in a subsequent experiment. Following the continuous illumination period, (i) the attenuation coefficient was measured, (ii) the laser beam was blocked for 30 min, and (iii) the attenuation coefficient was measured again. There was no difference in the coefficient measured before and after blocking the laser, which showed that the decline was irreversible. Since "thermal recovery" did not take place, photobleaching appears to be the primary cause of the decrease in attenuation coefficient during continuous, high-intensity illumination. However, the impact on a typical IOW−ATR experiment performed in our laboratory would be insignificant. In a typical experiment, the incident laser power is ≤5 mW and the total time that the sample is illuminated rarely exceeds 1 min. Thus, over the course of an experiment, a decline of less than 0.1% in the waveguide attenuation coefficient would be expected due to UO_2^{2+} photobleaching. This is an order of magnitude lower than the standard error of the attenuation measurement itself.

Conclusions

Sol−gel derived planar waveguides doped with UO_2^{2+} were prepared and characterized. A comparison of methods for determining waveguide attenuation coefficients by digital photography was performed. It was found that imaging UO_2^{2+} fluorescence excited by the propagating waveguide mode is a more precise method than imaging scattered light (Figures 3 and 4). In addition, both imaging methods were used to determine the attenuation coefficient of a waveguide-supported heme protein monolayer. The fluorescence method was clearly superior with respect to precision (Figure 5). Use of this method will enable attenuation measurements of very weakly absorbing, waveguide-supported films to be performed with significantly improved precision. As an example, UO_2^{2+}-doped waveguides have been used to perform absorbance linear dichroism measurements on a 0.3 monolayer film of hydrated yeast cytochrome *c*.[16] These measurements would have been problematic using the scattered light imaging method.

Finally, an additional advantage of the fluorescent imaging method is that it allows one to use waveguides of lower optical quality, which contain several scattering centers, for IOW−ATR experiments. For example, consider the waveguide represented by the scattered light attenuation data plotted in curve A of Figure 4. This waveguide would be unsuitable for IOW−ATR measurements on a thin molecular film using the scattered light imaging method, and consequently would not have been used in our past work.[6−8,15,16] However, as curve B in Figure 4 suggests, this waveguide would be suitable for such measurements when the fluorescence imaging method is employed. Consequently the fraction of sol−gel derived waveguides fabricated in our laboratory that are usable for IOW−ATR experiments has increased since the fluorescence imaging method was implemented.

Acknowledgment. We thank Elizabeth Gabbard for assistance in performing the bleaching measurements. This work was supported by the National Science Foundation (Grant CHE-9403896) and the National Institutes of Health (Grant R29 GM50299).

CM970429Y

(25) Mendes, S.; L. Li, L.; Burke, J.; Lee, J. E.; Saavedra, S. S. *Langmuir* **1996**, *12*, 3374.